Accepted Version

Wideband Untilted Narrow Wall Slotted Partially-Staggered Waveguide Array Based on Metalized Molded Plastic at E-band

Alejandro Garcia-Tejero, Fernando Rodríguez Varela, Roberto Torres-Sánchez, Mateo Burgos-Garcia and Francesco Merli

***Abstract*—A slotted waveguide antenna for automotive MIMO radar at 76-81 GHz consisting of a linear array with radiating untilted slots in the waveguide narrow wall is presented. Novel electrically large shared protrusions ($> \lambda_0/2$) in the waveguide walls to perturb transversal currents for high polarization purity while holding TE_{10} transmission properties and maintaining manufacturing constraints for millimetre-wave high-volume production are proposed. The design consists of only two layers of metallized plastic fabricated with injection molding, physical vapor deposition (PVD), electroplating, and soldering processes. Details about design methodology, electromagnetic simulations, and manufacturing process are disclosed. Prototyping confirms the feasibility of the proposed antenna concept at E-band and its outstanding performance, with an impedance bandwidth above 13.1%, 90% (-0.5 dB) of radiation efficiency at 78.5 GHz and a high cross-polar discrimination (28 dB).**

***Index Terms*—Waveguide, antenna array, untilted slot, narrow wall, metallized plastic, automotive radar, E-band.**

I. Introduction

Millimetre-wave automotive radars are based on digital beamforming (DBF) systems, which consist of several subarrays with moderate gain connected to integrated circuits (IC) [1]. Waveguide or gap waveguide [2], [3] antennas are promising candidates for this application due to their low-loss for long feeding networks and broadband impedance matching. Nonetheless, waveguides are challenging to fabricate cost-efficiently at high frequencies. Numerous well performing examples on milling [4], [5], micro-machining [6], [7], or 3D printing [8], [9] are available. However, these technologies are unsuitable for mass production. A promising alternative combines plastic injection molding and plating, achieving a low weight and high efficiency [10]–[12].

Narrow wall slot waveguide arrays enable to minimize spacing between antenna elements for DBF. In this case, the slots are usually tilted to be excited, and the inclination controls their coupling [13], [14]. However, this tilt creates an undesired cross-polar component, reducing efficiency significantly for small linear arrays (see Fig. 1). Multiple researchers have tackled this topic previously. Dudley [15] and Elliott [16] proposed placing electrically small obstacles ($\lambda_0/10$) on each side of the slots, which modified the currents flow, enabling untilted slots and low cross-polar. Unfortunately, this method is unfeasible at 77 GHz. Ghasemi [18], and Li [19] suggested using metal fences on the top surface surrounding the slots, reducing by 8 dB the cross-polar component, while adding $\lambda_0/4$ of extra thickness. Kildal [20] and Herranz [21] proposed adding parasitic metallic strips on dielectric plates; at the expense of causing additional losses at high frequencies. Sakakibara [10], [22] introduced the first narrow wall arrays at 77 GHz, obtaining good results for 2D arrays using protrusions below the slots. Their concept is constrained to λ_g spacing between slots to radiate in phase, which for 2D arrays can be solved by interleaving columns, whereas for linear arrays, it causes grating lobes. This work proposes an outperforming and cost effective solution to these limitations at millimetre-wave frequencies.

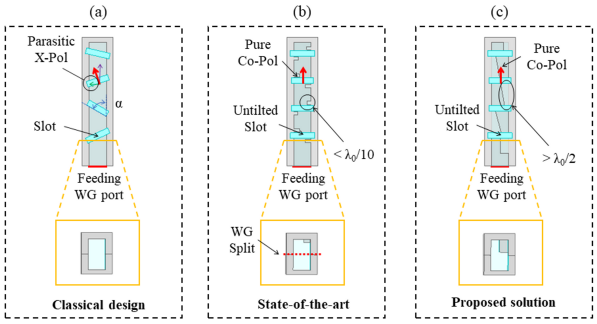

Fig. 1. The proposed antenna architecture compared to prior art. Longitudinal over transversal views, with metal in gray scale and blues for vacuum.

This letter presents a novel metalized plastic untilted narrow-wall slotted waveguide linear array design suitable for 76-81 GHz automotive MIMO radar. As illustrated in Fig. 1, the design comprises innovative electrically large protrusions ($> \lambda_0/2$), which alter the surface currents to enable untilted slot radiation while remaining manufacturable at E-band. An elementary unit analysis has been performed and confirmed by measurements on prototypes of the antenna array.

II. Elementary Slot Waveguide

The elementary unit of the proposed antenna is depicted in Fig. 2(a). The waveguide cell has been split in the center of the broad wall where currents are zero to ensure robustness

Alejandro Garcia-Tejero and Mateo Burgos-Garcia are with the Microwave and Radar Group, Department of Signals, Systems and Radiocommunications, ETSI Telecomunicación, Universidad Politécnica de Madrid, 28040 Madrid, Spain. Fernando Rodriguez Varela is with Universidad Rey Juan Carlos de Madrid, 28340 Madrid. Roberto Torres-Sánchez, Francesco Merli and Alejandro Garcia-Tejero are with HUBER+SUHNER AG, Herisau 9000 Switzerland. (e-mail: alejandro.garciatejero@hubersuhner.com).

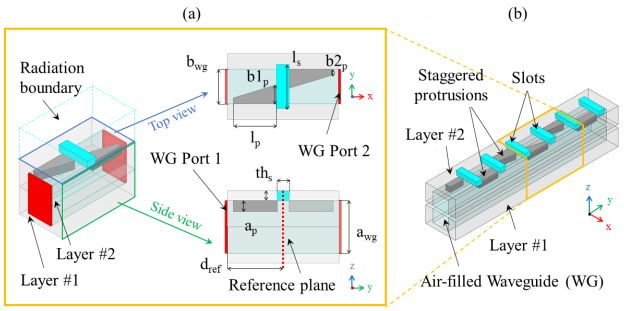

Fig. 2. (a) Representation of the elementary slot waveguide model. (b) Schematic of linear end-fed waveguide slot array.

to tolerances and minimize losses [18]. The upper layer of the waveguide contains two protrusions or insets to enhance the excitation of the radiating slot radiation by perturbing the surface currents of the TE_{10} mode. Both insets are characterized by their constant depth (a_p) and length (l_p) along the array, as well as by their linearly varying widths. These variations are defined in the longitudinal direction and by two taper parameters ($b1_p$ and $b2_p$), one per protrusion. The taper parameters allow an independent adjustment of the excitation of every radiating slot. Each inset is shared by two adjacent radiators, as shown in Fig. 2(b), and its length is determined by the separation between the slots, which is around half a guided wavelength ($\lambda_g/2$).

A. Slot coupling

Resonant narrow wall slot array antennas can be modeled as a transmission line where each slot is equivalent to a shunt admittance. The normalized admittance Y/Y_0 can be derived from the scattering parameters of the elementary unit waveguide of Fig. 2(a) [23], [24]:

$$Y/Y_0 = G + jB = \frac{-2S_{11}}{1+S_{11}} \tag{1}$$

where S_{11} is obtained by deembedding both feeding ports to the slot center. The slot radiates the power dissipated by the admittance in the circuit model, so the value of Y/Y_0 influences the matching and the array's excitation coefficients.

Y/Y_0 has been computed for several combinations of protrusion dimensions. The slot length is set to resonate at $f_0 = 78.5$ GHz, $l_s = \lambda_0/2$. The thickness th_p is 0.5 mm, the minimum achievable for the manufacturing technique. The waveguide cross-section dimensions a_{wg}, b_{wg} are set to 1.4 mm $\times$ 2.8 mm, between WR-10 and WR-12 standards.

Fig. 3 (a) and (b) depict the real and imaginary parts respectively of the admittance as a function of the protrusion height and width at f_0. The conductance is very low for $a_p/a_{wg} <$ 0.15. For $a_p/a_{wg} \in$ (0.15 - 0.25), variations in $b1_p$ directly impact the conductance, leading to a wide range from 0 to 0.8, representing an ideal operational area. When $a_p/a_{wg} > 0.25$, the conductance drops, showing that the slot no longer behaves as a shunt admittance. The imaginary part shows varying values due to the combination of the susceptances of the slot and inset. The values in the optimal operational region are

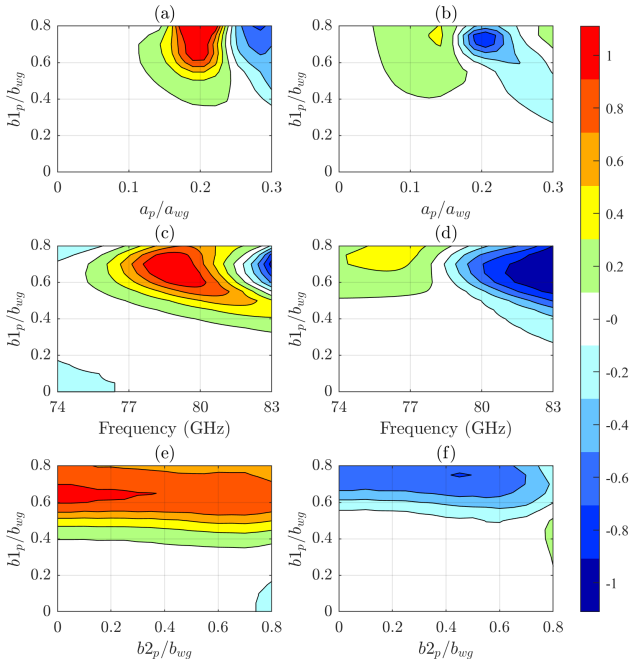

Fig. 3. Parametric results of normalized slot conductance (left column) and susceptance (right column) for different insets sizes.

mainly inductive due to the discontinuity introduced by the protrusion in the narrow wall [25].

The frequency dependence of the admittance is studied in Fig. 3(c) and (d). In this case, an optimal value of $a_p = 0.2a_{wg}$ is fixed to work in the ideal operation range area. Around f_0, the conductance is maximum while the susceptance is almost null, similar to a conventional waveguide slot [23]. As $b1_p$ increases, the resonance is slightly shifted to lower frequencies. This effect has already been observed for broad wall slots when exciting the slot with high levels of radiation [24].

In all previous experiments, $b2_p$ was set equal to $b1_p$. Now, the effect of the protrusion tapering is investigated by independently changing both parameters, as shown in Fig. 3(e) and (f). The conductance variations are dominated by $b1_p$, the dimension closer to the slot, while the effect of $b2_p$ is negligible. This is a desired behavior since, when designing the entire array, the admittance of a given slot can be adjusted without influencing the neighboring ones sharing the same protrusion. The susceptance also grows with $b1_p$ while being unaffected by $b2_p$, except when the latter takes values higher than $0.7b_{wg}$, where it adds a residual capacitance.

B. Waveguide propagation

The transmission line model for slotted waveguide arrays is valid as long as the propagation of the TE_{10} is not altered. Due to the large dimension of the proposed protrusions, a dedicated study has been performed to ensure that the dispersion characteristics of the waveguide remain unaffected within the operating bandwidth. The analysis simulates a periodic waveguide with varying protrusion dimensions without the slots.

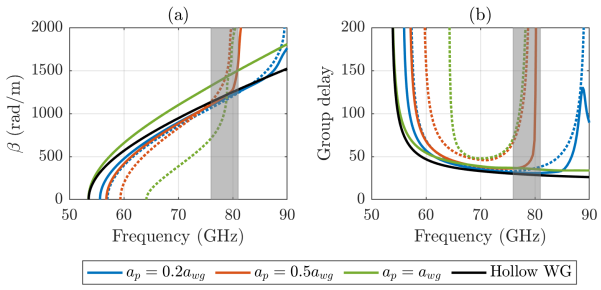

Fig. 4. Propagation characteristics of the proposed waveguide for variations of a_p with $b1_p = b2_p = 0.3b_{wg}$ (solid) and $b1_p = b2_p = 0.7b_{wg}$ (dotted).

Fig. 4 (a) shows the dispersion diagram for several combinations of a_p and $b1_p$, maintaining $b1_p = b2_p$. A stable dispersion curve against variations of $b1_p$ is desired since this parameter adjusts the slot excitation in the design process. Good stability is obtained for the optimal value of a_p $(0.2a_{wg})$, where β is identical to a hollow waveguide independently of the inset width. The protrusion modifies the propagation for high frequencies, introducing a high dispersion outside the operating band at 85 GHz. For larger values of a_p, the protrusion alters the fundamental mode with different effects depending on the value of $b1_p$. For instance, for $a_p = a_{wg}$ and $b1_p = 0.3b_{wg}$, the propagation exhibits a linear slope with low dispersion; however, when $b1_p = 0.7b_{wg}$ the mode becomes highly dispersive. The group delay depicted in Fig. 4 (b) helps to appreciate slope differences better.

III. Complete Antenna Design

A 6-slot sub-array antenna has been designed following the requirements of automotive MIMO front radar: directive elevation and moderately broad azimuth enabling DBF [1]. Typically, these sensors comprise several sub-arrays connected to a common IC. Fig. 5 depicts an exploded 3D view of the proposed antenna with the top and bottom views of the single layers. Three main functional elements can be distinguished:

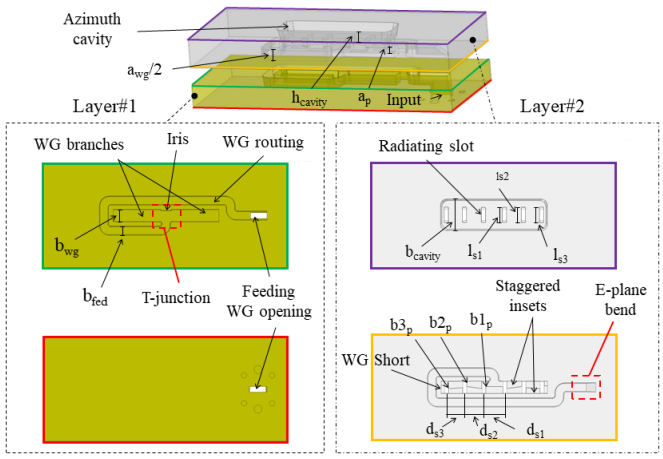

Fig. 5. Representation of the geometry of the proposed slotted waveguide array antenna and the bottom and top view of both Layer#1 and Layer#2.

A. Feeding section

The antenna is fed through a waveguide opening at the bottom, which in a commercial sensor is the interface to a coupling element connected to the IC [1]. An E-plane waveguide bend connects the port with a routing waveguide section tied to the linear sub-array. The routing length affects the antenna efficiency and has been set to 40 mm, a typical value in commercial sensors where the IC interface is not immediately close to the array location [26]. Finally, a T-junction incorporates a septum, which matches the array, removing all slots' combined susceptance.

B. Slotted waveguide

The antenna implements a center feeding scheme based on a T-junction for bandwidth enhancement. The equivalent circuit of the array is two identical waveguide branches of 3 parallel slots, each branch in series with the feeding line. The total admittance of each branch must be 2, so when combined in series, they match the transmission line admittance [23], [24].

Additionally, the normalized slot admittances (Y_i/Y_0) on each branch are adjusted to obtain the desired radiation pattern on the elevation plane using array synthesis techniques. Typically, automotive sub-arrays require a low side-lobe level (SLL) pattern which can be achieved with an amplitude tapering of the slot excitations. Another desired characteristic is the absence of deep nulls in the +/-20º range to maximize the antenna field-of-view (FOV). Therefore, a slight linear phase variation along slots is applied to remove the first null of the elevation pattern.

The normalized admittance values are translated to protrusion dimensions with the help of the conducted analytical studies and a further optimization process. Fig. 6 shows the electric field of the optimized structure at different sections. The amplitude and phase of each slot are appreciated in the cut XZ-plane.

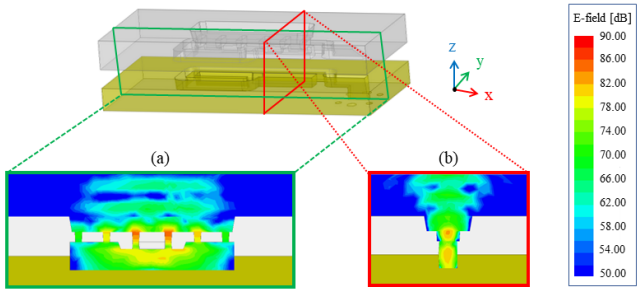

Fig. 6. Electric field for different cuts of the proposed array. (a) XZ-plane (Elevation plane), (b) YZ-plane (Azimuth plane).

C. Azimuth Cavity

Azimuth plane radiation pattern is adjusted with a cavity on top of the array. The cavity focuses the field radiated by the slots into a larger equivalent aperture, as shown in Fig. 6(b). Increasing b_{cavity} reduces the azimuth beamwidth and with h_{cavity} the phase error of the aperture can be controlled. The two parameters are used to adjust the half-power beamwidth (HPBW) of the array to 48º.

IV. Manufacturing and Experimental Results

The linear subarray consists of two plastic layers fabricated by injection molding. A deviation in the plastic expansion coefficient for the molding process was identified, making the parts larger by around 2%. Later, both pieces were metalized employing physical vapor deposition (PVD) and silver electroplating. Finally, the two metalized plastic layers were soldered together. The entire process was carried out at HUBER+SUHNER facilities [26]. The front and back views of the individual layers are shown in Fig. 7.

Fig. 7. Front and back views of each metallized plastic layer of the fabricated prototype.

Fig. 8 compares the measured results of the prototype, the simulation of the nominal design and two scaled versions (98% and 102%). Due to the variation in the plastic expansion, the waveguide air was reduced by the same amount. It can be seen how the good agreement of the scaled 98% simulation with the measured results. The reflection coefficient is lower than –15 dB in the 76-81 GHz band and below -10 dB between 73 to 82.6 GHz (13.1% of relative bandwidth).

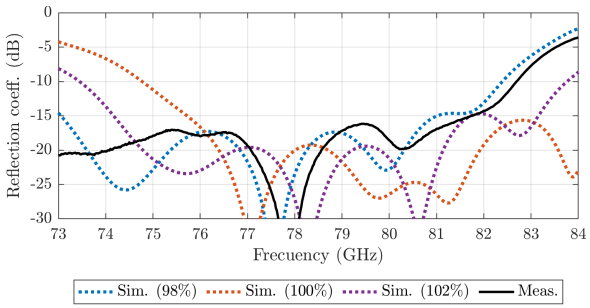

Fig. 8. Simulated reflection coefficient for nominal, scaled versions, and measurements of the manufactured prototypes.

The measured and simulated results of the radiation pattern in the elevation and azimuth planes at 76, 78.5 (f_0), and 81 GHz for the co-polar and cross-polar components are shown in Fig. 9. The elevation plane exhibits a narrow beam with a HPBW of 13°, 14° and 12° and a SLL of -22 dB, -20 dB and -19 dB respectively. The results exhibit very good agreement with simulations. Additionally, Fig. 8(d) displays the total efficiency over frequency, which is higher than 90% (-0.5 dB), and the maximum of cross-polarization discrimination level (XPD) in both radiation planes, going from 30 dB at 76 GHz to 28 dB at 81 GHz proving the design effectiveness.

To reflect the advantages of the proposed antenna design to the previous state-of-the-art a comparison is presented in Table II. This work excels in terms of total efficiency, especially considering the length of additional waveguide routing. The achieved XPD is consistent with narrow wall slotted waveguide antennas in literature. Notably, this result was obtained at a higher frequency or with a smaller array, which poses significant design challenges. Additionally, the presented solution outperforms impedance bandwidth benchmarks from the existing literature, all while employing a simplified two-layer design with integrated waveguide routing.

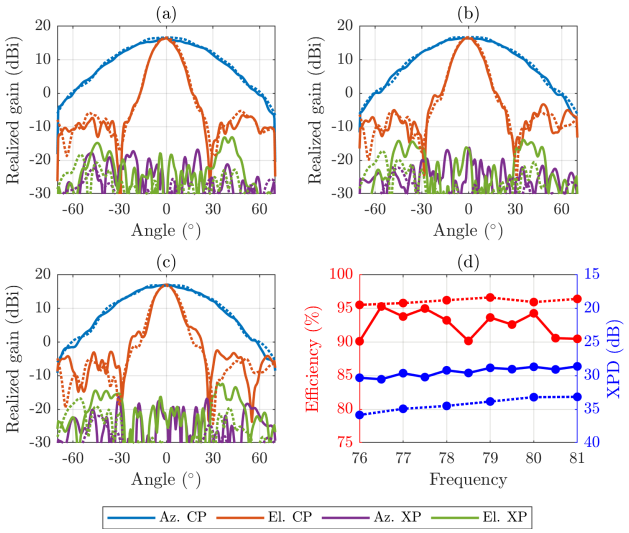

Fig. 9. Measured (-) and simulated (- -) co-polar and cross-polar radiation pattern at (a) 76, (b) 78.5, and (c) 81 GHz. (d) Total efficiency and XPD.

TABLE I
Comparison with previous works

Reference	[4]	[5]	[10]	[17]	[19]	[22]	This work
Feeding	BR	BR	NW	NW	NW	NW	NW
# of layers	2	3	2	2	3	2	2
f_o (GHz)	94	77	77	17	35	77	78.5
BW (%)	3.0	6.4	7.7	11.7	8.5	24.2	13.1
Polarization	V	H	H	V+H	V	45	V
XPD (dB)	-	-	29	33	25	29	28
G (dBi)	23.5	16.0	19.8	24.1	19.9	33.2	16.4
ϵ (%)	85	-	72	65	70	56	90

Note: BR broad wall waveguide, NW narrow wall waveguide, f_o operation frequency, BW relative impedance bandwidth (at -10 dB), G realized gain, and ϵ total efficiency.

V. Conclusion

In this letter, a slotted waveguide array with untilted narrow-wall slots has been presented. The design comprises novel electrically large protrusions within the waveguide walls, shared among neighbouring slots, enhancing polarization purity while maintaining compatibility with high-volume production. A prototype has been manufactured using only two layers of metalized plastic fabricated with injection molding, electroplating, and soldering processes. The measurement results showed a 13.1% impedance bandwidth, an XPD higher than 28 dB, and a total efficiency above 90%. Therefore, the proposed prototype serves as proof-of-concept for high efficiency, large bandwidth, and cost-efficient antenna suited for automotive MIMO radar at 77 GHz.

REFERENCES

[1] J. Hasch, E. Topak, R. Schnabel, T. Zwick, R. Weigel and C. Waldschmidt, "Millimeter-Wave Technology for Automotive Radar Sensors in the 77 GHz Frequency Band," in IEEE Transactions on Microwave Theory and Techniques, vol. 60, no. 3, pp. 845-860, March 2012.

[2] F. J. Sanchez Vazquez and R. Pearson, "Waveguide," European Patent, no. 1331688, Jan. 29 2002.

[3] P.-S. Kildal, E. Alfonso, A. Valero-Nogueira, and E. Rajo-Iglesias, "Local metamaterial-based waveguides in gaps between parallel metal plates," IEEE Antennas and Wireless Propagation Letters, vol. 8, pp. 84–87, 2009.

[4] J. Yue, C. Zhou, K. Xiao, L. Ding and S. Chai, "W-Band Low-Sidelobe Series-Fed Slot Array Antenna Based on Groove Gap Waveguide," in *IEEE Antennas and Wireless Propagation Letters*, vol. 22, no. 4, pp. 908-912, April 2023.

[5] Q. Ren, C. Bencivenni, G. Carluccio, H. T. Shivamurthy, A. De Graauw, F. Jansen, J. Yang, and A. U. Zaman, "Gapwaveguide automotive imaging radar antenna with launcher in package technology," IEEE Access, vol. 11, pp. 37 483–37 493, 2023.

[6] Y. Wang, M. Ke, M. J. Lancaster and J. Chen, "Micromachined 300-GHz SU-8-Based Slotted Waveguide Antenna," in IEEE Antennas and Wireless Propagation Letters, vol. 10, pp. 573-576, 2011, doi: 10.1109/LAWP.2011.2158285.

[7] D. Wang et al., "W-Band Low-SLL Size-Reduction Microwaveguide Array Antenna Using TE120-Mode-Cavity Dual-Layer Power Divider," in IEEE Antennas and Wireless Propagation Letters, vol. 20, no. 11, pp. 2146-2150, Nov. 2021, doi: 10.1109/LAWP.2021.3106657.

[8] J. Tak, A. Kantemur, Y. Sharma and H. Xin, "A 3-D-Printed W-Band Slotted Waveguide Array Antenna Optimized Using Machine Learning," in *IEEE Antennas and Wireless Propagation Letters*, vol. 17, no. 11, pp. 2008-2012, Nov. 2018.

[9] K. Lomakin, S. Alhasson and G. Gold, "Additively Manufactured Amplitude Tapered Slotted Waveguide Array Antenna With Horn Aperture for 77 GHz," in *IEEE Access*, vol. 10, pp. 44271-44277, 2022.

[10] Y. Hirayama, K. Sakakibara, H. Umemura, K. Miyazaki and N. Kikuma, "Effect of Wall-Surrounded Slot on Stepped Narrow Wall for Bandwidth Enhancement of Partially Parallel-Feeding Waveguide Traveling-Wave Array," in *IEEE Transactions on Antennas and Propagation*, vol. 65, no. 8, pp. 3976-3985, Aug. 2017

[11] T. Uesaka et al., "Design of Edge-Slotted Waveguide Array Antenna Manufactured by Injection-Molding," in *2019 IEEE International Symposium on Phased Array System & Technology (PAST)*, Waltham, MA, USA, 2019, pp. 1-4.

[12] A. Garcia-Tejero, M. Burgos-Garcia and F. Merli, "High-Efficiency Injection-Molded Waveguide Horn Antenna Array for 76-81 GHz Automotive Radar Applications," in *2022 19th European Radar Conference (EuRAD)*, 2022, pp. 21-24

[13] B. Das, J. Ramakrishna and B. Sarap, "Resonant conductance of inclined slots in the narrow wall of a rectangular waveguide," in *IEEE Transactions on Antennas and Propagation*, vol. 32, no. 7, pp. 759-761, July 1984.

[14] T. Li, H. Meng and W. Dou, "Design and Implementation of Dual-Frequency Dual-Polarization Slotted Waveguide Antenna Array for Ka-Band Application," in *IEEE Antennas and Wireless Propagation Letters*, vol. 13, pp. 1317-1320, 2014.

[15] D. Dudley, "An iris-excited slot radiator in the narrow wall of rectangular waveguide," in *IRE Transactions on Antennas and Propagation*, vol. 9, no. 4, pp. 361-364, July 1961

[16] S. Hashemi-Yeganeh and R. S. Elliott, "Analysis of untilted edge slots excited by tilted wires," in IEEE Transactions on Antennas and Propagation, vol. 38, no. 11, pp. 1737-1745, Nov. 1990.

[17] H. Luo, Y. Xiao, X. Lu and H. Sun, "Design of a Dual-Polarization Single-Ridged Waveguide Slot Array With Enhanced Bandwidth," in *IEEE Antennas and Wireless Propagation Letters*, vol. 18, no. 1, pp. 138-142, Jan. 2019.

[18] A. Ghasemi and J. -J. Laurin, "Beam Steering in Narrow-Wall Slotted Ridge Waveguide Antenna Using a Rotating Dielectric Slab," in *IEEE Antennas and Wireless Propagation Letters*, vol. 17, no. 10, pp. 1773-1777, Oct. 2018.

[19] Li, Teng Dou, Wenbin, "Design of an Edge Slotted Waveguide Antenna Array Based on T-Shaped Cross-Section Waveguide," in *International Journal of Antennas and Propagation*, 2017.

[20] J. Hirokawa and P. . -S. Kildal, "Excitation of an untilted narrow-wall slot in a rectangular waveguide by using etched strips on a dielectric plate," in *IEEE Transactions on Antennas and Propagation*, vol. 45, no. 6, pp. 1032-1037, June 1997.

[21] J. I. Herranz Herruzo, A. Valero-Nogueira, S. Martínez Giner and A. Vila Jiménez, "Untilted Narrow-Wall Slots Excited by Parasitic Dipoles in Groove Gap Waveguide Technology," in *IEEE Transactions on Antennas and Propagation*, vol. 63, no. 11, pp. 4759-4765, Nov. 2015.

[22] A. Mizutani, K. Sakakibara, N. Kikuma and H. Hirayama, "Grating Lobe Suppression of Narrow-Wall Slotted Hollow Waveguide Millimeter-Wave Planar Antenna for Arbitrarily Linear Polarization," in *IEEE Transactions on Antennas and Propagation*, vol. 55, no. 2, pp. 313-320, Feb. 2007.

[23] G. Stern and R. Elliott, "Resonant length of longitudinal slots and validity of circuit representation: Theory and experiment", in IEEE Transactions on Antennas and Propagation, vol. 33, no. 11, pp. 1264-1271, November 1985.

[24] R. V. Gatti, L. Marcaccioli and R. Sorrentino, "Design of slotted waveguide arrays with arbitrary complex slot voltage distribution," IEEE Antennas and Propagation Society Symposium, 2004., Monterey, CA, USA, 2004, pp. 3265-3268 Vol.3.

[25] David M. Pozar *Microwave Engineering*. Hoboken, NJ :Wiley, 2012.

[26] U. Huegel, A. Garcia-Tejero, R. Glogowski, E. Willmann, M. Pieper and F. Merli, "3D Waveguide Metallized Plastic Antennas Aim to Revolutionize Automotive Radar" in *Microwave Journal*, vol. 65, no. 9, September, 2022.